Water Supply

IWA PUBLISHING

Water Supply Vol 23 No 4, 1658 doi: 10.2166/ws.2023.095

Effects of highly corrosive pipe wall and disinfectant constituent on the chlorine decay behavior in drinking water

Kai Ma[a], Chuan Yu[b,*], Wenxi Xie[c] and Dongmei Fan[d]

[a] Tianjin Waterworks Group Co., Ltd, Tianjin 300040, China
[b] Tianjin Eco-Environmental Monitoring Center, Tianjin 300191, China
[c] Qiqihar Environmental Monitoring Station, Qiqihaer 161005, China
[d] Qiqihaer City Longsha District Agricultural Comprehensive Service Centre, Qiqihaer 161005, China
*Corresponding author. E-mail: 68413469@qq.com

KM, 0000-0002-7808-9557

ABSTRACT

In this study, a pilot-scale pipeline reactor and refined total chloramine decay model were employed to study the effects of the highly corrosive pipe wall and three kinds of disinfectant constituents on the chlorine decay behavior. The bulk decay coefficient, k_{bulk} for NaClO, NaClO + $NH_3{\cdot}H_2O$, and NaClO + $(NH_4)_2SO_4$ were 0.011, 0.004, and 0.004 h^{-1}, respectively. By resorting to the refined total chloramine decay model, the comprehensive wall decay coefficient k_{wall} appeared in the ascending order of NaClO, NaClO + $NH_3{\cdot}H_2O$, and NaClO + $(NH_4)_2SO_4$. The remarkable contribution of the aged cast iron pipe wall to overall total chlorine residual decay was manifested by the ratio, k_{wall}/k_{bulk}. The pipe wall-induced decay was related to microbe consumption and electrochemical corrosion as indicated by variations in total organic carbon (TOC), NO_2^--N, NO_3^--N, and Fe residual. The larger k_{wall} for NaClO + $NH_3{\cdot}H_2O$ (0.720 h^{-1}) relative to NaClO (0.465 h^{-1}) was mainly attributed to enhanced nitrifier-mediated microbe consumption. The largest k_{wall} for NaClO + $(NH_4)_2SO_4$ (0.864 h^{-1}) was due to the further promoted microorganism regrowth and metabolization as evidenced by the SO_4^{2-} declining behaviors. On this basis, it was suggested to minimize extra inorganic salt introduction into treated water to constrain microbial development in drinking water distribution system (DWDS). Temporal-free chlorine disinfection was also recommended for the chloraminated DWDS before the critical temperature.

Key words: biofilm, cast iron pipe, chlorine decay, disinfection strategy, drinking water distribution system

HIGHLIGHTS

- The new refined total chloramine decay model could well simulate total chlorine residual (TCR) decay behavior and give calibrated k_{wall}.
- TCR decay in aged cast iron (CI) pipe is caused by Fe-related corrosion and biotic consumption.
- Minimize inorganic salt introduction is recommended to maintain the TCR level in DWDS.

GRAPHICAL ABSTRACT

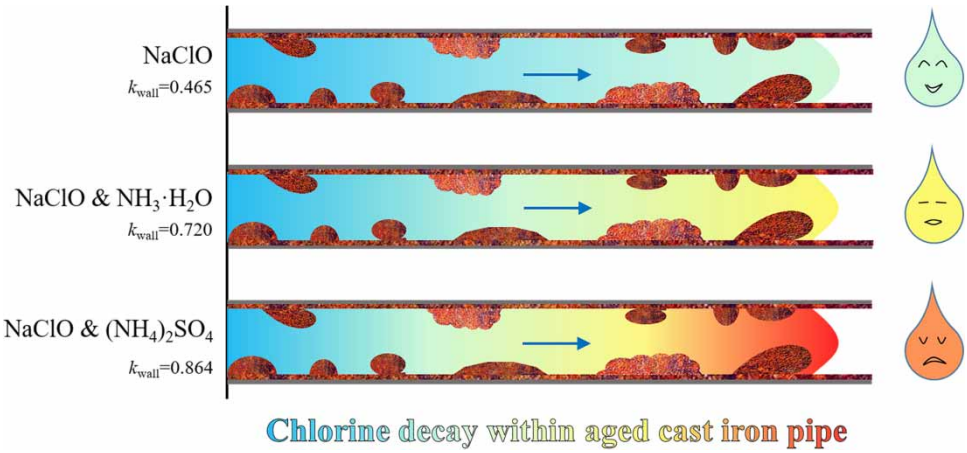

1. INTRODUCTION

The drinking water quality would get better than source water after a series of treatment in the drinking water treatment plant (DWTP). The treated water would be delivered to the thousands of households by resorting to the DWDS. The long-used pipelines could serve as biochemical reactor and make water quality deterioration to different extents, which depends on pipe materials and service age. This phenomenon is particularly significant for the stagnant water points or end points within the distribution system. Even active disinfection is widely taken by dosing chlorine-containing disinfectant, and the pipe wall-induced water quality deterioration could not be fundamentally avoided.

Chlorine-containing disinfectant could kill or inactivate microorganisms, so their residual level has become the key water quality index concerned by relevant regulators. It is reported that total chlorine residual (TCR) decay behavior may be remarkably different for the commonly used pipe materials. Digiano & Zhang (2005) developed a bench-scale pipe section reactor and found that free chlorine decay in the cast iron pipe is faster than that in the cement-lined ductile iron pipe. What is more, the model calculation results showed that wall-induced TCR decay accounts for a larger proportion relative to the loss in the bulk phase. With the help of the same reactor, the cast iron pipe was found to force chloramine to decay faster than cement-lined ductile iron pipe, and the chloramine decay was three orders of magnitude faster than bulk decay in the presence of cast iron pipe (Westbrook & Digiano 2009). A water quality model was developed in EPANET to model the full-scale DWDS in the town of Goderich, and it was found that the largest impacts are from the unlined cast iron pipe and lesser impacts are progressively from the ductile pipe and then polyvinylchloride pipe (Huang & McBean 2008). Another field study on chloraminated distribution systems further corroborated that unlined cast iron pipe consumes chloramine more severely than epoxy-lined cast iron pipe and PVC pipe (Liu *et al.* 2015). Therefore, aged cast iron pipe serves as the main cause to the disinfectant decay in the full-scale water distribution system.

The cast iron pipe is characterized by a rough inner wall consisting of iron tuberculation and attached biofilms (Li *et al.* 2014). On encountering fresh bacteria, chlorine/chloramine could oxidize cellular membranes, nucleic acid, and other living matters until it is killed, which is the fundamental purpose of using disinfectant in the field of DWDS. Besides, the microorganism within the biofilm can also produce, release, and accumulate extracellular polymeric substances to protect microbes from disinfectants and toxic materials as a response to chloramine stress (Herath & Sathasivan 2020). Hence, the existence of biofilm attached to the pipe wall would necessarily consume disinfectant to some extent depending on the total biomass and metabolic activity. On the other hand, the exposed zero-valent iron can reduce chlorine/chloramine to Cl^- in the way of an electrochemical reaction, which appears to be a disinfectant-consuming process as well (Li *et al.* 2014). The complicated surface composition makes the cast iron pipe wall act as a 'black hole' to intensively consume free chlorine or combined chlorine. In fact, the surface composition could be reshaped in response to the disinfectant constituent and concentration. It is reported that chloramine disinfection is more prone to stimulate nitrifiers to grow on the pipe wall (Hua *et al.* 2011) and produce dense crystallized particles (Li *et al.* 2014) relative to chlorine disinfection.

Once established in biofilms, nitrifiers can be difficult to eliminate by solely increasing chloramine concentrations, as the nitrifiers are relatively resistant to the dissolved chloramine by releasing soluble microbial products (Krishna *et al.* 2012). However, free chlorine could stop biofilm development in organic carbon-limited water (Chandy & Angles 2001). Considering the adaptability of biofilm to the specific disinfectant (Shen *et al.* 2016), periodic free chlorine maintenance has been suggested and applied in chloraminated water supply systems to stop nitrification (Hua *et al.* 2011). The reaction of surface composition to disinfectant alteration should be further defined for the aged CI pipe to put forward applicable water treatment and system management strategies.

Actually, many utilities have now switched from chlorine gas and liquid ammonia to sodium hypochlorite (NaClO) and ammonium sulfate ($(NH_4)_2SO_4$), respectively, due to security concerns. The impact of transition in disinfectant constituent on pipe wall composition and further on the disinfectant decay behavior is still in the course of clarification. To investigate the effects of aged CI pipe wall and disinfectant constituent on the chlorine decay behavior, the bulk decay behavior was studied using brown glass bottles for NaClO, $NaClO + NH_3{\cdot}H_2O$, and $NaClO + (NH_4)_2SO_4$. A pilot-scale pipeline reactor was constructed and employed to study the overall TCR decay behaviors in response to the three kinds of disinfectant constituents. The contributions of the CI pipe to overall decay were quantified by using the newly developed refined total chloramine decay model (RTCDM). On the basis, the changes in pipe wall composition and corresponding TCR decay behavior were summarized for different disinfectant constituents. Finally, disinfection strategies were tentatively proposed for the chloraminated water supply system.

2. MODEL DEVELOPMENT

Chlorine and chloramine are active reagents and can participate in many biochemical reactions within the drinking water supply system. On the basis of the extensive research on disinfection chemistry, chloramine decay in water could be classified into bulk phase decay and pipe wall-induced decay. The bulk phase decay could be further ascribed to disinfectant autodecomposition and oxidizing reductive compounds, e.g., natural organic matter (NOM) and bioprotein. Every single reaction pertinent to chloramine autodecomposition has been fully characterized under different pH and temperature values (Vikesland *et al.* 2001; Huang 2008). The oxidation of NOM by chloramine and chlorine could be described as the biphasic second-order kinetic model with four specific reaction parameters (Duirk *et al.* 2005). On this basis, Wahman (2018) and Ricca *et al.* (2019) packaged the aforementioned two components into the prediction model to simulate TCR decay behavior in the batch reactor. The chloramine decay model and corresponding reaction rates for the prediction model could be obtained by reference to the previously published articles (Wahman 2018; Ricca *et al.* 2019). Besides, nitrite could also be oxidized by chloramine in the bulk phase (Margerum *et al.* 1994), which is more prominent in nitrified DWDS. Moreover, it has long been observed that pipe wall-induced chloramine decay accounts for much of the overall loss (Rossman *et al.* 1994; Huang & McBean 2008). As a result, we incorporated the nitrite oxidation component and pipe wall consumption component into the prediction model and developed the total chloramine decay model (TCDM) in our previous study (Ma *et al.* 2020). When used in a real distribution system, the TCDM returned satisfying prediction results on TCR decay behavior.

As for an aqueous solution, chloramine concentration is in chemical equilibrium with that of chlorine. The trace chlorine existing in water would manifest its significant effect on TCR decay when there is no pipe wall-induced consumption. It is found that chlorine experiences autodecomposition to produce ClO_3^- or O_2, which is temperature, pH, and NH_4^+-N dependent (Adam *et al.* 1992; Adam & Gordon 1998). Therefore, the monochloramine hydrolysis reaction and chlorine autodecomposition model were incorporated into the original TCDM to better describe the TCR decay behavior in chloraminated water with trace chlorine. The RTCDM consisting of 23 differential equations for kinetic reactions and 4 algebraic equations for equilibrium reactions was edited in C programming language on MATLAB software (version R2018b) and solved using differential algebraic equations solver ode15s. The RTCDM can return the calibrated wall decay coefficient with its computing core using the nonlinear least square approximation method.

The wall decay coefficients were calibrated using RTCDM based on three sets of water quality data obtained from pipeline reactor experiments. As for the bulk phase decay experiments, the bulk decay coefficients were obtained by fitting the experimental data to the pseudo-first-order kinetic model, which was also edited in C programming language on MATLAB software (version R2018b). The curve fitting calculation would stop only until the size of the gradient is less than the value of the optimality tolerance.

3. MATERIALS AND METHODS

3.1. Bulk phase decay experiments

To isolate the pipe wall consumption from overall TCR decay, bulk phase decay experiments were carried out by filling brown glass bottles with prepared feed water (NaClO, NaClO + $NH_3{\cdot}H_2O$, NaClO + $(NH_4)_2SO_4$). Parallel experiments were conducted simultaneously for each feed water. Six to eight samples were collected from 0 to 48 h for each experiment. TCR, alkalinity, pH, water temperature, NH_4^+-N, NO_2^--N, TOC, and SO_4^{2-} were determined for each sample. The data used in model calculation are the average value of the two data from the parallel experiments.

3.2. Pipeline reactor experiments

To evaluate the contribution of the pipe wall to the overall TCR decay, a pipeline reactor was employed and operated in a continuous flow mode. The reactor mainly consists of a water tank (~300L) with a stirrer, an integrated controller, three pumps with different flow rates and corresponding float flowmeters, a target pipeline, a stainless support frame, and valves as shown in Figure 1. The flowrate of feed water could be effectively controlled within the range of 0–12 $m^3{\cdot}h^{-1}$. The target pipeline, with a diameter ϕ ranging from 50 to 200 mm, could be flexibly replaced and fixed on the reactor by a pipe fixator. Here, six sections of highly corrosive CI pipes were taken from full-scale DWDS (Tianjin, China), each of them having a diameter of 100 mm and a length of 1 m. They were installed on the reactor in a cascade form.

On installation, the inner wall of CI pipes has to get dried with many tuberculations unevenly spaced in the pipe. Hence, we initiated the reactor on 15 April 2020 with treated water to reestablish the microbial community in the pipeline at the flowrate of 6.2 $m^3{\cdot}h^{-1}$, which is similar to that in DWDS. During the 83-day operation, the feed water was refreshed every 2 days. The formal TCR decay experiment was started on 7 July 2020 using fresh treated water. After a 3-day operation, the reactor was stopped, and the experimental water was drained out. Then the filtered water was fed into the system followed by the immediate addition of 2 $mg{\cdot}L^{-1}$ NaClO (aq). As the pipe wall severely consumed chlorine disinfectant, TCR was increased to 2 $mg{\cdot}L^{-1}$ by adding NaClO (aq) every 2 h. After a 24-h cleaning by free chlorine, the water was drained out and fresh filter water was fed into the system to conduct the formal TCR decay experiment with chlorinated water. After a 3-day operation, the water was drained out, and another 30-day operation was conducted by feeding fresh treated water every 2 days to promote microbes' adaptability to the chloraminated water once again. Subsequently, the last formal TCR decay experiment was carried out with fresh filtered water chloraminated by $NH_3{\cdot}H_2O$ for 3 days. The operational procedure of the pipeline reactor could be seen in Figure S1.

For every formal experiment, the reactor was operated under the same flowrate of 6.2 $m^3{\cdot}h^{-1}$. The sample was collected after the first 3 min of circulation and that time was set as the start point. The samples were collected at the operation

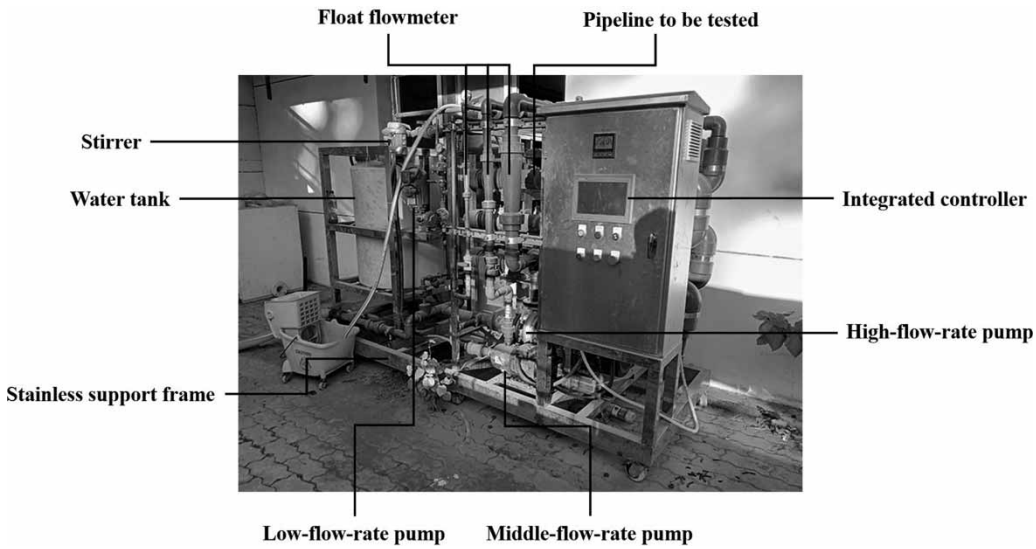

Figure 1 | Schematic of a pipeline reactor.

time of 0, 1, 4, 8, 24, 48, and 72 h. TCR, pH, alkalinity, water temperature, NH_4^+-N, NO_2^--N, NO_3^--N, TOC, Fe residual, and SO_4^{2-} were measured.

3.3. Feed water preparation and analytical methods

The treated water was obtained from Lingzhuang DWTP (Tianjin, China), adopting prechlorination (NaClO), coagulation, flocculation, settling, dual media filtration, and final chloramination by $(NH_4)_2SO_4$. The treated water was used directly as the $NaClO + (NH_4)_2SO_4$ water in the bulk phase decay experiments and pipeline reactor experiments. The filtered water was used as the NaClO water. $NaClO + NH_3{\cdot}H_2O$ was prepared by adding $NH_3{\cdot}H_2O$ into filtered water. The properties of feed water are presented in Table 1. TCR was measured by the *N*, *N*-diethyl-p-phenylenediamine method with a portable colorimeter (DR300, HACH, USA). pH was tested by a pH meter (S210-K, METTLER TOLEDO, Switzerland). Total alkalinity was determined by the acid–base indicator titration method according to the Water and Wastewater Monitoring Analysis Method. By using the UV–Visible spectrophotometer (DR6000, HACH, USA), NH_4^+-N was determined by the salicylate method at the wavelength of 655 nm with a resolution of 0.01 mg·L^{-1}, NO_2^--N was determined by the diazotization method at the wavelength of 507 nm with a resolution of 0.001 mg·L^{-1}, NO_3^--N was determined by the Cd reduction method at the wavelength of 507 nm with a resolution of 0.01 mg·L^{-1}, SO_4^{2-} was determined by the Barium sulfate precipitation method at the wavelength of 450 nm with a resolution of 1 mg·L^{-1}, and Fe residual was determined by 1, 10-phenanthroline method at the wavelength of 510 nm with a resolution of 0.01 mg·L^{-1}. TOC was determined by the TC-IC method using a TOC analyzer (TOC-L, Shimadzu, Japan). The gross α and β radioactivities were measured by using evaporation, concentration, and enumeration methods.

3.4. Data input strategy

For the bulk phase decay experiments, only the time series data of TCR were input into the pseudo-first-order kinetic model to conduct parameter (k_{bulk}) calibration. As for the pipeline reactor experiments, seven parameters listed in Table 1 (except Fe residual, SO_4^{2-}, Gross α radioactivity, and Gross β radioactivity) were set as the initial conditions in RTCDM. The time series data of TCR were also input into the RTCDM to achieve parameter (k_{wall}) calibration. Upon model calculations, the effects of pipe wall and disinfectant constituent on TCR decay could be quantitatively reflected by comparing k_{bulk} and k_{wall}.

4. RESULTS

4.1. Chlorine decay in bulk phase

Bulk phase decay is the reduction in TCR in bulk water irrespective of the pipe wall effect. The gross α and β radioactivities of the water were relatively constant during the three experiments, and Figure 2 shows the variations in TCR in the bulk phase.

Table 1 | Properties of feed water used in the six sets of experiments

	Bulk phase decay experiments			Pipeline reactor experiments		
Parameters	**$NaClO + (NH_4)_2SO_4$**	**NaClO**	**$NaClO + NH_3{\cdot}H_2O$**	**$NaClO + (NH_4)_2SO_4$**	**NaClO**	**$NaClO + NH_3{\cdot}H_2O$**
Temperature (°C)	26.1	25.9	26.7	27.3	28.1	27.3
pH	7.730	7.959	7.928	7.620	7.826	7.719
Alkalinity (mg·L^{-1})	80	85	80	80	82	85
TCR (mg·L^{-1})	1.35	1.62	1.53	1.23	1.59	1.11
NH_4^+-N (mg·L^{-1})	0.44	0.00	0.40	0.47	0.00	0.33
NO_2^--N (mg·L^{-1})	0.004	0.002	0.004	0.007	0.002	0.003
TOC (mg·L^{-1})	1.50	1.50	1.50	1.88	2.14	1.50
SO_4^{2-} (mg·L^{-1})	35	33	32	35	33	32
Fe residual (mg·L^{-1})	*N*[a]	*N*[a]	*N*[a]	0.08	0.04	0.05
Gross α radioactivity (mBq·L^{-1})	30	31	32	21	21	22
Gross β radioactivity (mBq·L^{-1})	77	78	77	73	73	73

[a]Fe residual was not measured for the corresponding feed water.

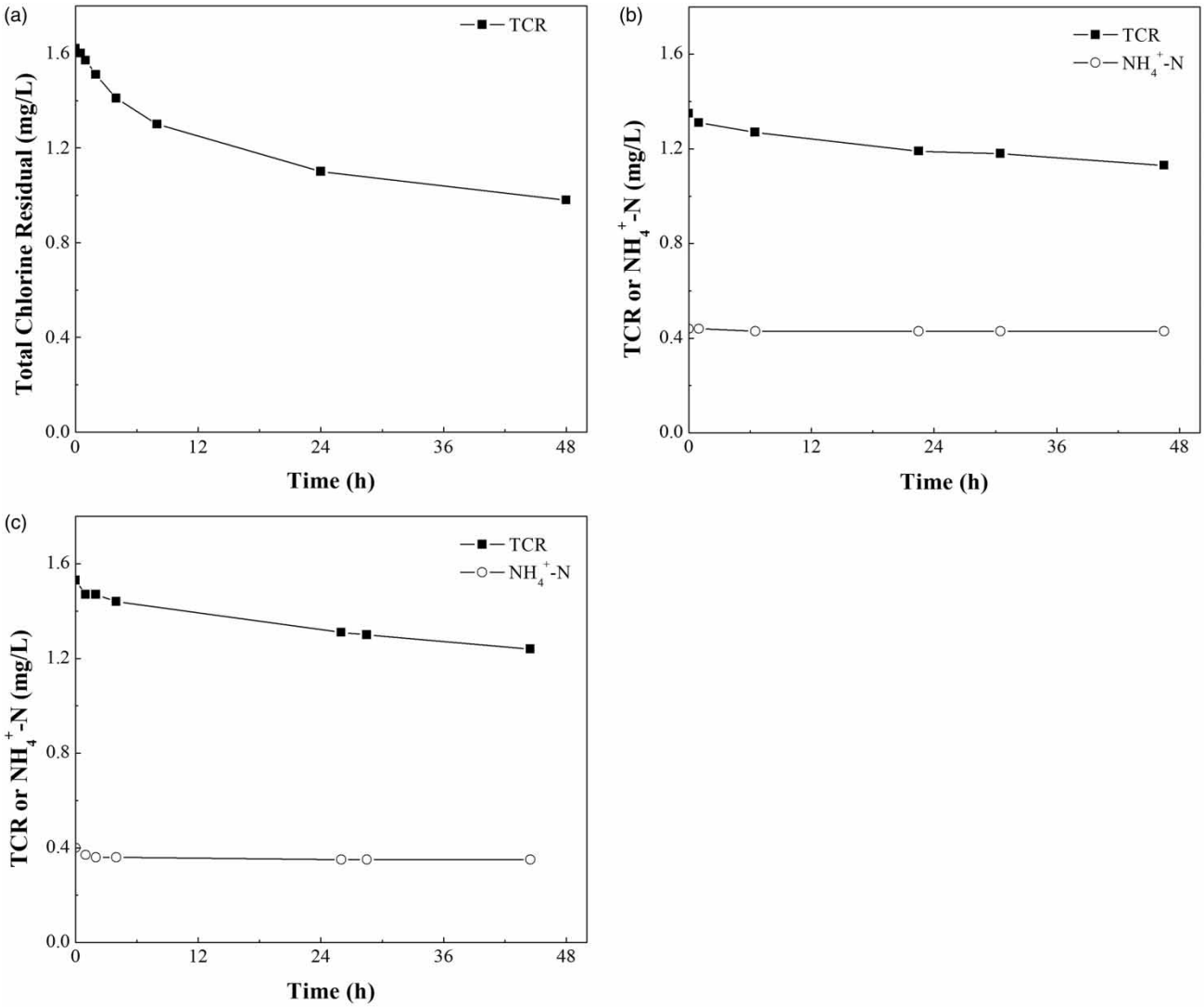

Figure 2 | Variations in total chlorine residual and NH_4^+-N with time in bulk phase. (a) NaClO group, (b) NaClO + $(NH_4)_2SO_4$ group, and (c) NaClO + $NH_3{\cdot}H_2O$ group.

For the three sets of disinfectant constituent studied here, TCR all decreased with time in a deceleration mode. Especially, by comparing Figure 2(a) with Figure 2(b) and (c), the free chlorine experiment was characterized by the higher TCR descent rate, while the two chloramine experiments had visually the similar TCR descent rate. Figure 2 also presents the changes in NH_4^+-N in the course of TCR decay. The NH_4^+-N concentration all stepped into the stable state after the gentle decrease in the early stage for the two experiments chloraminated by NaClO + $(NH_4)_2SO_4$ and NaClO + $NH_3{\cdot}H_2O$. Hence, the changes in ammonium salt did not have obvious impacts on TCR and NH_4^+-N variation behavior in bulk water.

4.2. Chlorine decay within circulation pipeline reactor

TCR decay within the circulation pipeline reactor includes the bulk phase decay and pipe wall-induced disinfectant decay simultaneously. The gross α and β radioactivities of the water were also relatively constant which were the same as the bulk phase decay experiments, and Figure 3 shows the variations in TCR within the pipeline reactor. Compared with bulk phase decay experiments shown in Figure 2, the pipeline reactor experiments had the features of a higher descent rate, no matter for chlorinated water or chloraminated water. Concretely, they had an extremely faster decrease speed within the first 4–6 h and then shifted to the slow a decline stage. Figure 3 also presents the changes in NH_4^+-N in the course of TCR

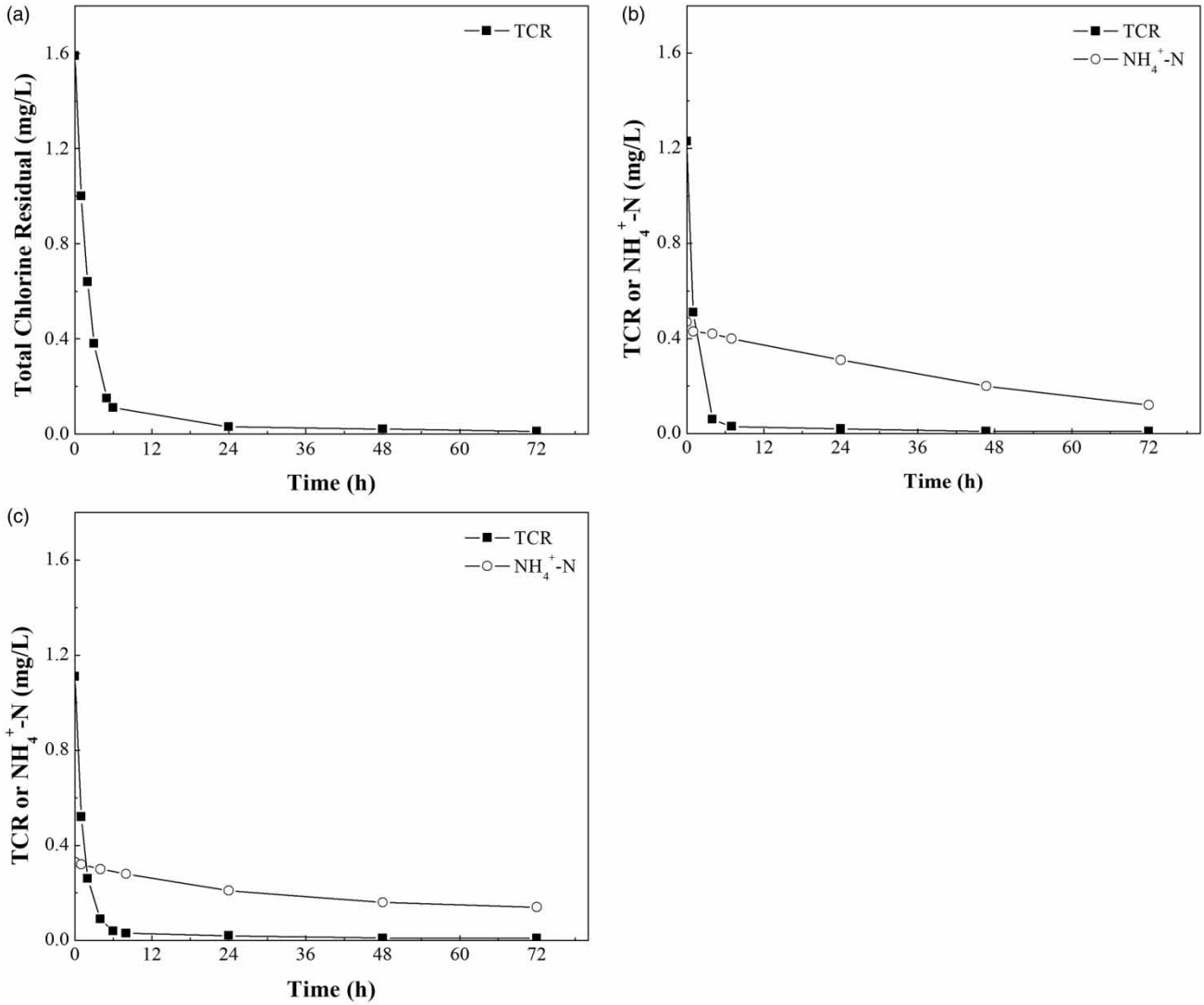

Figure 3 | Variations in total chlorine residual and NH_4^+-N with time in pipeline reactor. (a) NaClO group, (b) $NaClO + (NH_4)_2SO_4$ group, and (c) $NaClO + NH_3{\cdot}H_2O$ group.

decay. As shown in Figure 3(b) and (c), NH_4^+-N decreased all the way to the end of about 0.12–0.14 $mg{\cdot}L^{-1}$ for the two sets of experiments chloraminated by $NaClO + (NH_4)_2SO_4$ and $NaClO + NH_3{\cdot}H_2O$, which is very different from those of bulk phase decay experiments. In other words, the highly corrosive pipes used here greatly reshaped the disinfection chemistry, which would be further discussed in Section 5.

5. DISCUSSION

5.1. Pipe wall effect dominates?

To what extent did the pipe wall affect the disinfectant chemistry is the first question that needs to be answered. The data from bulk phase decay experiments were fitted to the pseudo-first-order kinetic model. Figure 4 gives the simulation results for the three sets of experiments. It could be seen that the fitting lines fit the experimental results well with the goodness of fit of 0.939, 0.898, and 0.957 for $NaClO + (NH_4)_2SO_4$ system, NaClO system, and $NaClO + NH_3{\cdot}H_2O$ system, respectively. The larger slope of dashed line relative to the other two fitting lines means a higher TCR descent rate in chlorinated water.

The data from pipeline reactor experiments were input into RTCDM to conduct decay coefficient calibrations. Figure 5 gives the calibration results for the three sets of experiments. It could be seen that the calibration lines could ideally

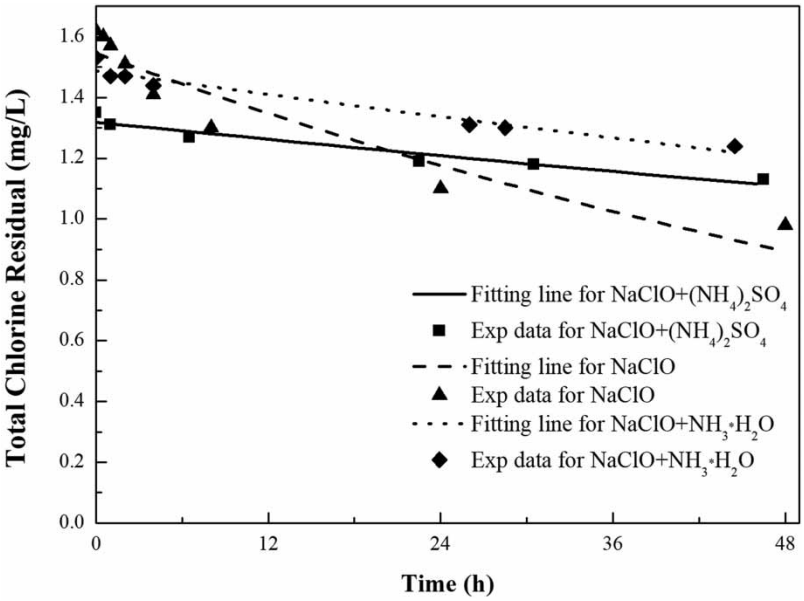

Figure 4 | Simulation results for the three sets of bulk phase decay experiments based on the pseudo-first-order kinetic model.

match the experimental results with the goodness of fit of 0.998, 0.999, and 0.996 for $NaClO + (NH_4)_2SO_4$ system, NaClO system, and $NaClO + NH_3{\cdot}H_2O$ system, respectively. To further visually compare the TCR decay behavior, the calibration lines within the first 12 h were zoomed in and figured in the inset of Figure 5. The solid line representing the $NaClO + (NH_4)_2SO_4$ system has the steepest slope at the early stage. When shifting from $(NH_4)_2SO_4$ to $NH_3{\cdot}H_2O$, the dotted line appears to be the smaller slope. By contrast, the dashed line is characterized by the smallest slope, which means that free chlorine disinfection has the smallest TCR descending speed among the three experiments.

The TCR decay coefficients obtained from model calibrations were tabulated in Table 2. The bulk decay coefficient k_{bulk} for the two chloramination experiments were all 0.004 h^{-1}, while the coefficient for the chlorination experiment was 0.011 h^{-1}, a

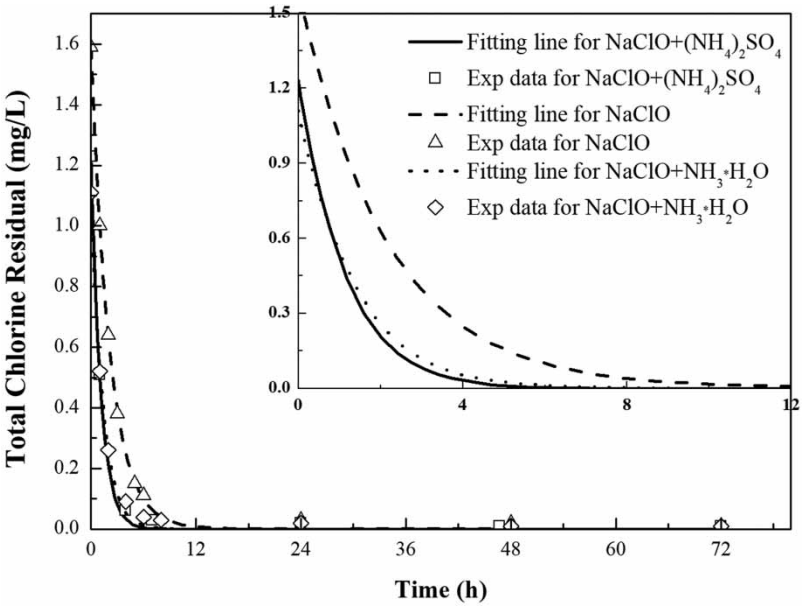

Figure 5 | Calibration results for the three sets of pipeline reactor experiments based on the RTCDM.

Table 2 | Summary of TCR decay coefficients obtained from RTCDM calibrations and pseudo-first-order kinetic model simulations

Disinfectant composition	k_{bulk} (h^{-1})	k_{wall} (h^{-1})	k_{wall}/k_{bulk}
$NaClO + (NH_4)_2SO_4$	0.004	0.864	216
$NaClO + NH_3{\cdot}H_2O$	0.004	0.720	180
NaClO	0.011	0.465	42

little bit larger than that of the former two. By calibrating the experimental data with RTCDM, the pipe wall-induced TCR decay was quantitatively isolated from the overall decay within the pipeline reactor. The comprehensive wall decay coefficient k_{wall} for the three pipeline reactor experiments was 0.465–0.864 h^{-1}. To evaluate the contribution to the overall decay, the ratio k_{wall}/k_{bulk} was calculated and shown in the last column in Table 2. The ratio ranged from 42 to 216; therefore, more than 97% of the overall decay could be explained by pipe wall consumption. In 2009, a pipe section reactor study, also using tuberculated cast iron pipe, calculated the k_{wall} of 0.597–0.709 h^{-1} (Westbrook & Digiano 2009), which is within the boundary of our calibration results. However, our recent field study on the Tianjin distribution network found that the k_{wall} was evidently smaller than the results presented here, and the ratio was only about 5.0–9.0, which depended on the season and distribution routine (Ma *et al.* 2020). These outcomes manifest that identical numerical results could hardly be obtained as the bench- and pilot-scale studies are easier to keep the physical and chemical conditions constant, which is not the case for the field study (variations in pipe material, water velocity). However, no matter for which scale, all these studies proved that the pipe wall could dominate the overall chloramine decay in the pipes, especially for the highly corrosive cast iron pipes.

Figure 6 shows the variations in TOC, NO_2^--N, and NO_3^--N for $NaClO + (NH_4)_2SO_4$ experiment. After a 83 d adaptive operation, accompanied by the constant decline in NH_4^+-N (Figure 3(b)), NO_2^--N experienced a continuous ascend in the first 24 h, followed by a constant decline in the last 48 h as shown by the solid triangle connected by the dashed line in Figure 6. NO_3^--N had a similar changing behavior, but its inflection point appeared at 4 h as shown by the hollow diamond connected by a dashed line in Figure 6. It could be inferred that nitrification bacterial had been considerably developed in the pipeline reactor and could utilize NH_4^+-N and NO_2^--N as the energy sources to produce NO_2^--N and NO_3^--N by ammonia-oxidizing bacteria and the nitrite-oxidizing bacteria, respectively (Hua *et al.* 2011). Peng *et al.* (2006) found that denitrification bacteria could be activated by precisely controlling the pH even down to 7.5 at anoxic conditions. Recently, a study using

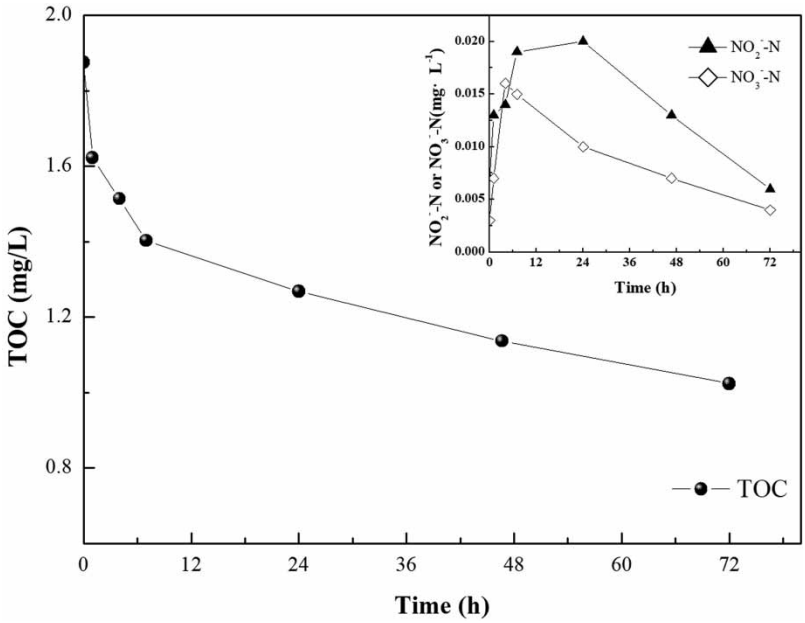

Figure 6 | Variations in TOC, NO_2^--N, and NO_3^--N for water chloraminated by NaClO and $(NH_4)_2SO_4$.

microelectrodes and confocal laser scanning microscopy found dissolved oxygen (DO) descended from DO > 8 mg·L^{-1} in the bulk phase to ~5 mg·L^{-1} in the biofilm cultured in the chloraminated water (Pressman *et al.* 2012). Another study detected denitrification activity under the corrosion scale as well (Nawrocki *et al.* 2010). The constant decline in TOC (shown in Figure 6) further proved the existence of denitrifier, sulfate-reducing bacteria (SRB), and other heterotrophic bacteria in our pipeline reactor. Inactivating these microbes and oxidizing chloramine decaying proteins (CDPs) excreted by microbes (Herath & Sathasivan 2020), would lead to the disinfectant decay.

Figure 7 shows the variations in Fe residual for the $NaClO + (NH_4)_2SO_4$ experiment. When starting the high-flowrate pump, the stark contrast in flow state drives the loosely attached debris to resuspend in the bulk water, which is manifested by the elevation in Fe residual from 0.08 (Table 1) to 0.83 mg·L^{-1}. As shown in Figure 7, Fe residual keeps ascending within the first hour. According to the Nernst equation under our physic-chemical conditions listed in Table 1, the second increase in Fe residual is the significant evidence of electrochemical corrosion between Fe and chloramine at the surface of the pipe wall (Equation (1)). The soluble product Fe^{2+} would be further oxidized by DO and chloramine and would transform into $Fe(OH)_3$ (Equations (2) and (3)). Under the steady flow state, the excessive insoluble $Fe(OH)_3$ would gradually precipitate on the surface of the pipe wall, which led to a continuous decrease within the last 71 h as shown in Figure 7. The disinfectant's effect on iron corrosion has been quantitatively studied with the index of corrosion rate (Treweek *et al.* 1985). They found that disinfection with chloramine in the range of 0.4–1.2 mg·L^{-1} resulted in corrosion rates of about 5 mg·dm^{2-}·d^{-1}, whereas disinfection with chlorine over the same range led to higher corrosion rates. So Fe/Fe^{2+}-mediated electrochemical corrosion is another cause driving disinfectant decay within the cast iron pipe employed in this study.

$$2H_2O + NH_2Cl + Fe \rightarrow NH_4^+ + Cl^- + Fe^{2+} + 2OH^- \quad (1)$$

$$2H_2O + NH_2Cl + 4OH^- + 2Fe^{2+} \rightarrow NH_4^+ + Cl^- + 2Fe(OH)_3 \downarrow \quad (2)$$

$$2H_2O + O_2 + 8OH^- + 4Fe^{2+} \rightarrow 4Fe(OH)_3 \downarrow \quad (3)$$

The contribution of microbe consumption and electrochemical corrosion to the TCR decay was not quantified in this study. But, the two pipe wall-relating factors have shown their significant effects on the chlorine/chloramine decay process, which is much stronger relative to the bulk decay. Given the highly corrosive pipe attached by well-developed biofilm, how the different compositions of disinfectants react to the pipe wall needs to be further addressed.

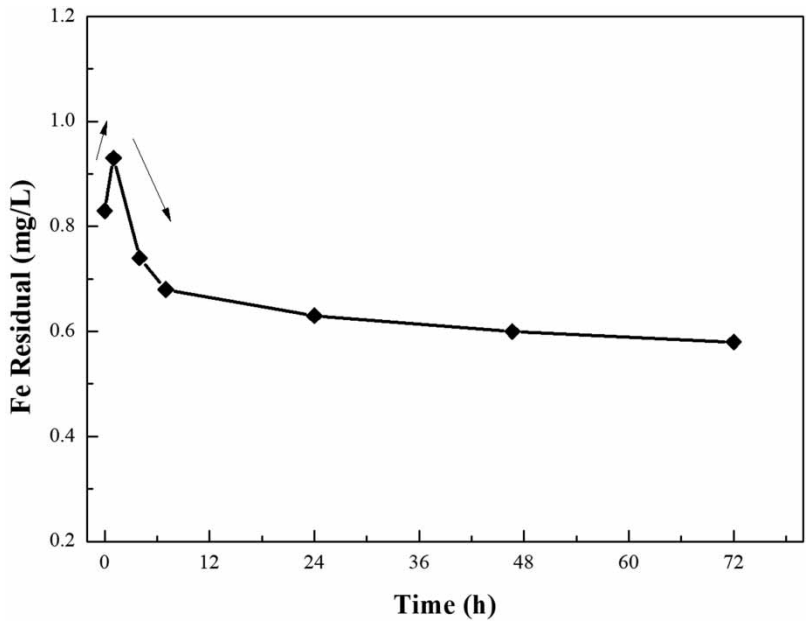

Figure 7 | Variation in Fe residual for water chloraminated by NaClO and $(NH_4)_2SO_4$.

5.2. Disinfectant composition affects chlorine decay?

In a real distribution system, different compositions of disinfectants are used. Here, NaClO, NaClO + $(NH_4)_2SO_4$, and NaClO + $NH_3{\cdot}H_2O$ were studied to compare their variation behaviors in bulk water and cast iron pipeline systems. As shown in Table 2, the bulk decay coefficients are the same for the two chloramination experiments. So the origins of NH_4^+-N ($(NH_4)_2SO_4$ or $NH_3{\cdot}H_2O$) would not obviously influence disinfectant decay dynamics in the bulk phase. Comparatively, the decay coefficient for NaClO disinfection is 2.75 times that of the former two. The accelerated decay behavior is the result of the faster autodecomposition of chlorine (Kulkarni *et al.* 2018) and the faster oxidation with NOM (Duirk *et al.* 2005) in the aqueous solution. Interestingly, the wall decay coefficient for NaClO disinfection is 0.465 h^{-1}, which is the smallest among the three experiments (Table 2). However, the decay coefficient for NaClO + $NH_3{\cdot}H_2O$ disinfection is 1.55 times that for free chlorine disinfection. The decay process further accelerated NaClO + $(NH_4)_2SO_4$ disinfection with a decay coefficient 0.86 times higher than that for chlorine disinfection. The reverse order in decay coefficient manifests the different reactions of the pipe wall to the disinfectant constituent, which could further lead to the different disinfectant decay behavior.

Even chloramine could better penetrate into the biofilm (Lee *et al.* 2011), NH_4^+-N produced upon inactivation or oxidation could serve as a nitrogen source to nitrifier and other bacteria (Hua *et al.* 2011), which may significantly boost bacteria reproduction within the pipeline. Comparatively, chlorine has the better microorganism inactivation ability and could effectively kill bacteria and prevent CDPs from producing and releasing by bacteria. As a result, the bacteria-mediated TCR decay could be directly slowed down upon free chlorine disinfection. What is more, it is reported that nitrification could remarkably decrease pH within the biofilm (Pressman *et al.* 2012). Under the low pH condition, Fe oxidizing bacteria could utilize Fe^{2+} to produce Fe^{3+}, which may speed up the iron corrosion process (Teng *et al.* 2008). On the other hand, it is found that free chlorine disinfection could stimulate iron release from the pipe wall obviously relative to chloramine disinfection (Li *et al.* 2014; Hu *et al.* 2018). Therefore, corrosion-relating TCR decay observed here was mainly attributed to the microorganism-mediated pathway. The different reactions of heavily polluted pipe wall to NaClO and NaClO + $NH_3{\cdot}H_2O$ cause the difference in the TCR decay behavior.

Besides the pH effect, the substitution of $NH_3{\cdot}H_2O$ by $(NH_4)_2SO_4$ would introduce additional SO_4^{2-} into the aqueous solution. The background SO_4^{2-} value is 32–33 mg·L^{-1}, and dosing $(NH_4)_2SO_4$ increases SO_4^{2-} by about 2 mg·L^{-1} (Table 1). Figure 8 shows the initial and the final concentrations of SO_4^{2-} of the three pipeline reactor experiments. For NaClO + $(NH_4)_2SO_4$ disinfection experiment, the largest amount of SO_4^{2-} (9 units) was consumed within the reactor during the 3-day operation. For NaClO + $NH_3{\cdot}H_2O$ disinfection experiment, 5 units of SO_4^{2-} was consumed. NaClO disinfection is characterized by the minimum SO_4^{2-} consumption (2 units). The SRB has been found to exist under the corrosion scale

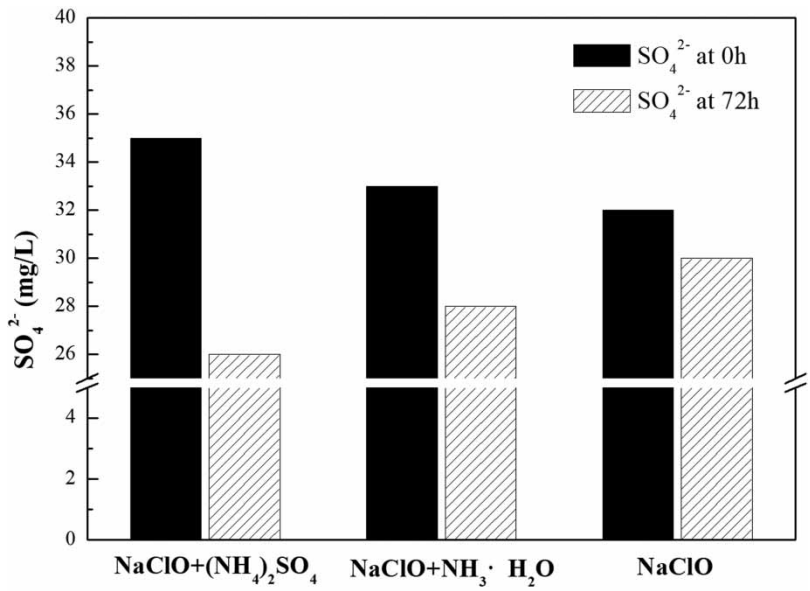

Figure 8 | Difference of the SO_4^{2-} declining behaviors among the three pipeline reactor experiments.

that has low DO and utilize SO_4^{2-} to produce S^{2-} (Lytle & Maynard 2005). Besides SRB, many other microbes could reproduce in a synthetic medium consisting of $(NH_4)_2SO_4$ and $MgSO_4$. So the SO_4^{2-} addition may encourage the microbes' reproduction and metabolism in the heavily polluted pipeline reactor.

The introduction of NH_4^+-N could stimulate the development of nitrifiers and other microbes within the attached biofilm. The additional SO_4^{2-} would further exacerbate the TCR decay problem by encouraging SRB and other microbes' reproduction and metabolism. Luckily, free chlorine disinfection could be used to cope with the problem with higher performance relative to combined chlorine disinfection.

5.3. What to do to maintain TCR level in distribution system?

Based on the aforementioned discussion, chlorine was found to be suitable for slowing down TCR decay and limiting microorganism development within the highly corrosive pipeline system. The introduction of NH_4^+-N or SO_4^{2-} has an adverse effect on the maintenance of the TCR level. Therefore, it is supposed to minimize NH_4^+ and SO_4^{2-} addition to drinking water delivered by the highly polluted cast iron pipe.

With the advance of technology, cement-lined ductile iron pipe is found to be inert in water chemistry with high strength. The cement-lined pipe is reported to have fewer effects on TCR decay for chloraminated water (Westbrook & Digiano 2009). Therefore, the long-used cast iron pipes are being replaced by the cement-lined pipes in recent years. The changes in pipe materials can reduce the disinfectant consumption in water mains. But the small diameter CI pipes left in community or buildings would still lead to the sharp drop in TCR for tap water, especially during the hot season (Ma *et al.* 2020). Besides disinfectant lost in DWDS, production safety may also affect decision-making on disinfection craft. For example, free chlorine and NH_4^+ are dosed in the form of NaClO and $(NH_4)_2SO_4$ instead of Cl_2 and $NH_3{\cdot}H_2O$, respectively, in some large-scale water supply systems in China (e.g., Beijing and Tianjin). In fact, the disinfection strategy is the result of the trade-off among water quality safety, practical feasibility, and low cost.

It should be noted that the evident biotic- and abiotic-mediated TCR decay has been broadly observed under the high water temperature, but it is not the case for the low water temperature. The retarded biochemical reaction under low temperature would be more compatible with chloramine disinfection. So a flexible disinfection strategy may be more suitable for the specific water supply system. The consistent free chlorine disinfection may be suitable for the small-scale DWDS or the DWDS having a large proportion of long-used CI pipe. For large-scale water supply systems, combined chlorine disinfection can be used to maintain TCR level throughout the DWDS, on the condition that only limited CI pipes are still in use. In that case, $NH_3{\cdot}H_2O$, instead of $(NH_4)_2SO_4$, is recommended to accomplish the chloramination to minimize the risk of stimulating microorganism regrowth. But if the water temperature is in transition to a high level, measures should be taken in advance to prevent microorganism boosting in DWDS. Given microbial problems typically are worse when pipeline water is 15 °C or higher (Neden *et al.* 1992), DWTP is supposed to switch to free chlorine disinfection to perform pipeline cleaning before the critical temperature comes. After which, DWTP can reuse the combined chlorine as the secondary disinfectant. This strategy has been adopted by some water supply systems, such as Pinellas county utilities in America (Hua *et al.* 2011) and Foshan city utilities in China (Deng *et al.* 2015). Overall, to constrain microorganism activity in chloraminated DWDS, it is recommended to reduce free ammonia levels in the entry-point by using high Cl_2:NH_3 ratios, carry out free chlorine maintenance timely by DWTP, replace the aged CI pipes, and flush the distribution pipes of low velocity. The usefulness of free chlorine maintenance has been substantiated for the highly corrosive pipes in this pilot study. Interestingly, NH_4Cl may serve as the optional composite to accomplish the treated water chloramination with the advantage of no extra inorganic salt introduction. Hence, its effectiveness on distribution pipes, especially for the aged CI pipes, could be evaluated in the future to see its advantages over $(NH_4)_2SO_4$.

6. CONCLUSIONS

The pipeline reactor was employed to study the effects of highly corrosive cast iron pipes on the disinfection chemistry at the pilot scale. The contributions of CI pipe under different compositions of disinfectants were quantified by using the refined TCDM. The key conclusions are as follows:

1. The newly developed RTCDM could well simulate TCR decay behavior based on the experimental data and give the calibrated k_{wall} to quantify the pipe wall contributions.

2. $NaClO + (NH_4)_2SO_4$ may promote microorganism regrowth and metabolization in CI pipe with unevenly spaced tuberculation, which further accelerates the TCR decay process. Comparatively, $NaClO + NH_3{\cdot}H_2O$ has the features of a smaller k_{wall} as no extra SO_4^{2-} introduction. Free chlorine could effectively inactivate or kill microorganism attached to the pipe wall, and as a result, the overall TCR decay process could be slowed down.
3. The forces driving TCR decay in highly corrosive CI pipe include iron-mediated electrochemical corrosion and microbe-mediated (e.g., nitrifier and SRB) biotic disinfectant consumption.
4. It is recommended to minimize extra inorganic salt introduction into treated water to constrain microbial development in DWDS. As for the chloramine disinfection system, DWTP could conduct free chlorine maintenance to clean the whole DWDS. Besides reducing the free ammonia level, replacing and flushing the distribution pipe may be beneficial for maintaining the TCR level.

ACKNOWLEDGEMENT

The authors acknowledge the funding offered by Tianjin Water Group Co. Ltd (Project Number: 2019KY-02). The authors would like to acknowledge PE. Fushou Wan of Tianjin Hongyuan Water Treatment Engineering Co., Ltd. for his help in providing us the insight into hydrodynamics. The authors also acknowledge Vice Manager Feng Xiao of Lingzhuang Water Treatment Plant in Tianjin for his help in providing the filtered and treated water.

DATA AVAILABILITY STATEMENT

All relevant data are included in the paper or its Supplementary Information.

CONFLICT OF INTEREST

The authors declare there is no conflict.

REFERENCES

Adam, L. C. & Gordon, G. 1998 Hypochlorite ion decomposition: effects of temperature, ionic strength, and chloride ion. *Inorganic Chemistry* **38** (6), 1299–1304.

Adam, L. C., Fabian, I., Suzuki, K. & Gordon, G. 1992 Hypochlorous acid decomposition in the pH 5–8 region. *Inorganic Chemistry* **31** (17), 3534–3541.

Chandy, J. P. & Angles, M. L. 2001 Determination of nutrients limiting biofilm formation and the subsequent impact on disinfectant decay. *Water Research* **35** (11), 2677–2682.

Deng, J. X., Kuang, J. Y., Deng, G. Y., Luo, X. M., Wen, S. X. & Pan, W. J. 2015 Control of residual chlorine reduction in chloramine disinfection network by chlorine disinfection method. *Water Technology* **9** (6), 22–26.

Digiano, F. A. & Zhang, W. 2005 Pipe section reactor to evaluate chlorine–wall reaction. *Journal-American Water Works Association* **97** (1), 74–85.

Duirk, S. E., Gombert, B., Croué, J. P. & Valentine, R. L. 2005 Modeling monochloramine loss in the presence of natural organic matter. *Water Research* **39** (14), 3418–3431.

Herath, B. S. & Sathasivan, A. 2020 The chloramine stress induces the production of chloramine decaying proteins by microbes in biomass (biofilm). *Chemosphere* **238**, 124526.

Hu, J., Dong, H., Xu, Q., Ling, W., Qu, J. & Qiang, Z. 2018 Impacts of water quality on the corrosion of cast iron pipes for water distribution and proposed source water switch strategy. *Water Research* **129**, 428–435.

Hua, G., Baggett, C., Hall, J., Powell, R., Reed, T., Friedrich, T. & Stasis, P. 2011 Controlling nitrification in a distribution system receiving blended multiple source waters: the experience of Pinellas County utilities. *Florida Water Resources Journal* **63** (12), 42–48.

Huang, X. C. 2008 *Reactions Between Aqueous Chlorine and Ammonia: A Predictive Model. Civil Engineering Dissertations*. Northeastern University, Boston, MA, USA.

Huang, J. J. & McBean, E. A. 2008 Using Bayesian statistics to estimate chlorine wall decay coefficients for water supply system. *Journal of Water Resources Planning and Management* **134** (2), 129–137.

Krishna, K. C. B., Sathasivan, A. & Sarker, D. C. 2012 Evidence of soluble microbial products accelerating chloramine decay in nitrifying bulk water samples. *Water Research* **46** (13), 3977–3988.

Kulkarni, V., Awad, J., van Leeuwen, J., Drikas, M., Chow, C., Cook, D., Medlock, A., Trolio, R. & Amal, R. 2018 Impact of zinc on biologically mediated monochloramine decay in waters from a field based pilot scale drinking water distribution system. *Chemical Engineering Journal* **339**, 240–248.

Lee, W., Wahman, D., Bishop, P. & Pressman, J. 2011 Free chlorine and monochloramine application to nitrifying biofilm: comparison of biofilm penetration, activity, and viability. *Environmental Science & Technology* **45** (4), 1412–1419.

Li, X., Wang, H., Zhang, Y., Hu, C. & Yang, M. 2014 Characterization of the bacterial communities and iron corrosion scales in drinking groundwater distribution systems with chlorine/chloramine. *International Biodeterioration & Biodegradation* **96**, 71–79.

Liu, M. J., Craik, S. & Zhu, D. Z. 2015 Determination of cast iron pipe wall decay coefficient for combined chlorine in a municipal water distribution system. *Canadian Journal of Civil Engineering* **42** (4), 250–258.

Lytle, D. A. & Maynard, T. L. G. B. 2005 Effect of bacterial sulfate reduction on iron-corrosion scales. *Journal-American Water Works Association* **97** (10), 109–120.

Ma, K., Hu, J., Han, H., Zhao, L., Li, R. & Su, X. 2020 Characters of chloramine decay in large looped water distribution system – the case of Tianjin, China. *Water Supply* **20** (4), 1474–1483.

Margerum, D. W., Schurter, L. M., Hobson, J. L. & Moore, E. E. 1994 Water chlorination chemistry: nonmetal redox kinetics of chloramine and nitrite ion. *Environmental Science & Technology* **28** (2), 331–337.

Nawrocki, J., Urszula, R.-S., Swietlik, J., Olejnik, A. & Miroslawa, J. S. 2010 Corrosion in a distribution system: steady water and its composition. *Water Research* **44** (6), 1863–1872.

Neden, D. G., Jones, R. J., Smith, J. R., Kirmeyer, G. J. & Foust, G. W. 1992 Comparing chlorination and chloramination for controlling bacterial regrowth. *Journal-American Water Works Association* **84** (7), 80–88.

Peng, Y. Z., Shao-Po, W., Shu-Ying, W., Jian-Ge, H. & Hai-Bing, Q. 2006 Effect of denitrification type on pH profiles in the sequencing batch reactor process. *Water Science & Technology* **53** (9), 87–93.

Pressman, J. G., Lee, W. H., Bishop, P. L. & Wahman, D. G. 2012 Effect of free ammonia concentration on monochloramine penetration within a nitrifying biofilm and its effect on activity, viability, and recovery. *Water Research* **46** (3), 882–894.

Ricca, H., Aravinthan, V. & Mahinthakumar, G. 2019 Modeling chloramine decay in full-scale drinking water supply systems. *Water Environment Research* **91** (5), 441–454.

Rossman, L. A., Clark, R. M. & Grayman, W. M. 1994 Modeling chlorine residuals in drinking-water distribution systems. *Journal of Environmental Engineering* **120** (4), 803–820.

Shen, Y., Huang, C. H., Monroy, G. L., Janjaroen, D., Derlon, N., Lin, J., Espinosa-Marzal, R., Morgenroth, E., Boppart, S. A., Ashbolt, N. J., Liu, W. T. & Nguyen, T. H. 2016 Response of simulated drinking water biofilm mechanical and structural properties to long-term disinfectant exposure. *Environmental Science & Technology* **50** (4), 1779–1787.

Teng, F., Guan, Y. T. & Zhu, W. P. 2008 Effect of biofilm on cast iron pipe corrosion in drinking water distribution system: corrosion scales characterization and microbial community structure investigation. *Corrosion Science* **50** (10), 2816–2823.

Treweek, G. P., Glicker, J., Chow, B. & Sprinker, M. 1985 Pilot-plant simulation of corrosion in domestic pipe meterials. *Journal-American Water Works Association* **77** (10), 74–82.

Vikesland, P. J., Ozekin, K. & Valentine, R. L. 2001 Monochloramine decay in model and distribution system waters. *Water Research* **35** (7), 1766–1776.

Wahman, D. G. 2018 Web-based applications to simulate drinking water inorganic chloramine chemistry. *Journal-American Water Works Association* **110** (11), 43–61.

Westbrook, A. & Digiano, F. A. 2009 Rate of chloramine decay at pipe surfaces. *Journal-American Water Works Association* **101** (7), 59–70.

First received 20 November 2022; accepted in revised form 31 March 2023. Available online 12 April 2023